ARTICLE OPEN ACCESS

Biallelic mutation of *HSD17B4* induces middle age–onset spinocerebellar ataxia

Yukiko Matsuda, PhD, Hiroyuki Morino, MD, PhD, Ryosuke Miyamoto, MD, Takashi Kurashige, MD, PhD, Kodai Kume, MD, PhD, Noriyoshi Mizuno, DDS, PhD, Yuhei Kanaya, MD, Yui Tada, MS, Ryosuke Ohsawa, PhD, Kazunori Yokota, MD, PhD, Nobuyuki Shimozawa, MD, PhD, Hirofumi Maruyama, MD, PhD, and Hideshi Kawakami, MD, PhD

Correspondence
Dr. Morino
morino@hiroshima-u.ac.jp

Neurol Genet 2020;6:e396. doi:10.1212/NXG.0000000000000396

Abstract

Objective

To determine the genetic underpinnings of slowly progressive spinocerebellar ataxia, autosomal recessive (SCAR), we performed exome analysis and examined the relationship between clinical severity and functional change induced by the mutation.

Methods

Homozygosity fingerprinting and exome sequencing were performed to identify causative mutations in 2 consanguineous families. We assessed the expression of D-bifunctional protein (DBP) and the amount of dimerized DBP in fibroblasts by immunoblot and quantitative reverse transcription PCR. The pathogenicity of the mutation was evaluated using the Combined Annotation-Dependent Depletion (CADD) scores; these results were compared with the scores of previously reported mutations.

Results

We identified a homozygous mutation as causative of middle age–onset SCAR: p.Ala175Thr, which is located in *HSD17B4* that encodes peroxisomal DBP. The patients developed cerebellar ataxia, and the subsequent progression was slow. The symptoms presented were milder than those in previously reported cases. The messenger RNA expression levels were normal, but protein levels were diminished. Dimerization of DBP was also reduced. The CADD score of the identified mutation was lower than those of previously reported mutations.

Conclusions

This is the report of middle age–onset DBP deficiency. Residual functional DBP caused relatively mild symptoms in the affected patients, i.e., slowly progressive ataxia and hearing loss. This study broadens the scope of DBP deficiency phenotypes and indicates that CADD scores may be used to estimate the severity of DBP deficiencies.

From the Department of Epidemiology (Y.M., H. Morino, K.K., Y.K., Y.T., R.O., H.K.), Research Institute for Radiation Biology and Medicine, Hiroshima University; Japan Society for the Promotion of Science (Y.M.), Tokyo; the Department of Clinical Neuroscience (R.M.), Institute for Biomedical Science, Tokushima University; the Department of Neurology (T.K.), National Hospital Organization Kure Medical Center and Chugoku Cancer Center; the Department of Periodontal Medicine (N.M.), Graduate School of Biomedical and Sciences, Hiroshima University; the Department of Plastic Surgery (K.Y.), Hiroshima University Hospital; the Division of Genomics Research (N.S.), Life Science Research Center, Gifu University; the Department of Clinical Neuroscience and Therapeutics (H. Maruyama), Hiroshima University, Japan.

Go to Neurology.org/NG for full disclosures. Funding information is provided at the end of the article.

The Article Processing Charge was funded by the authors.

Glossary

BN = blue native; **CADD** = Combined Annotation-Dependent Depletion; **DBP** = D-bifunctional protein; **IBD** = identity by descent; **mRNA** = messenger RNA; **PAGE** = polyacrylamide gel electrophoresis; **PDB** = Protein Data Bank; **RT-qPCR** = quantitative reverse transcription PCR; **SCAR** = spinocerebellar ataxia, autosomal recessive; **SNP** = single nucleotide polymorphism; **VLCFA** = very-long-chain fatty acid.

Homozygous or compound heterozygous mutations in *HSD17B4* (MIM #601860) are responsible for D-bifunctional protein (DBP) deficiency (MIM #261515), a disorder of peroxisomal fatty acid oxidation; very-long-chain fatty acids (VLCFAs) are one of the substrates of DBP. DBP has multiple enzymatic activities[1,2] and contains 3 domains: dehydrogenase, hydratase, and sterol carrier protein-2. DBP deficiency is classified into 3 subtypes (type I–III) depending on the affected domain and consequent enzymatic activity.[3] All types present during infancy as severe hypotonia, seizures, and dysmorphic features. Diagnosis is based on confirmation of elevated plasma VLCFA levels. Most patients with DBP deficiency die before age 2 years.

Mutations of the *HSD17B4* gene also cause juvenile-onset DBP deficiencies[4–8] and Perrault syndrome.[9–11] As both clinical phenotypes overlap and are less severe than those of infant-onset DBP deficiencies, patients with these disorders survive until adolescence/adulthood. Patients with juvenile-onset DBP deficiencies and Perrault syndrome present with hearing loss, cerebellar ataxia, peripheral neuropathy, infertility, and normal plasma VLCFA levels.

We describe patients with a slowly progressive spinocerebellar ataxia, autosomal recessive (SCAR) in middle age. Genetic analysis implicated *HSD17B4* as the causative gene. Although reports on juvenile-onset DBP deficiency with mild symptoms have increased, middle age–onset DBP deficiency has not been previously reported. We confirmed a reduction in DBP with in vitro assays and compared the severity of DBP deficiency with those caused by previously reported mutations.

Methods

Standard protocol approvals and patient consents

This study was approved by the Human Subjects Committees of Hiroshima University. Written informed consent was obtained from all subjects. Clinical details were collected from medical records and interviews.

Patients

We enrolled 2 Japanese families with autosomal recessive traits for cerebellar ataxia. Family 1 was from Kagawa, Shikoku; family 2 was from Kagoshima, South of Kyusyu. Families 1 and 2 included 3 and 2 affected individuals, respectively (figure 1A). Blood samples were obtained from 2 affected individuals in family 1 and from 2 affected and 3 unaffected individuals in family 2. All patients were diagnosed with slowly progressive spinocerebellar ataxia by neurologists. Before this study, we confirmed that all affected individuals had no pathogenic mutations of SCA1, 2, 3, 6, 7, 8, 31, 36, and dentatorubral-pallidoluysian atrophy.

Homozygosity fingerprinting, exome sequencing, and variant filtering

Single nucleotide polymorphism (SNP) genotyping was performed using the Genome-Wide Human SNP Array 6.0 (Affymetrix, Santa Clara, CA). We used homozygosity fingerprinting to obtain the identity by descent (IBD).[12] Exome sequencing was performed using 2 samples from patients, 1-IV-2 and 2-IV-1 (figure 1A), as previously described.[13] More than 100,000 variants in each sample were called. We filtered the candidate variants based on open databases (dbSNP v151, the 1000 Genomes Project, and Exome Sequencing Project), genomic position, function, and zygosity. Variants observed in the in-house database were excluded. We selected the variants localized in the region isolated from the homozygosity fingerprinting. Functional predictions due to amino acid changes were estimated using PolyPhen-2,[14] SIFT,[15] MutationTaster,[16] and the Combined Annotation-Dependent Depletion (CADD).[17] All reported genomic coordinates were in GRCh37/hg19. Candidate variants were confirmed by Sanger sequencing (ABI3130; Thermo Fisher Scientific, Waltham, MA).

Cell culture

Skin biopsies were performed to obtain fibroblasts from 2 patients, 1-IV-2 and 2-IV-1, and from healthy controls. Fibroblasts were grown in Dulbecco Modified Eagle Medium, containing 10% fetal bovine serum, 100 U/mL of penicillin, and 100 μg/mL of streptomycin, under humidified air at 37°C in 5% CO_2.

Western blotting

Fibroblasts were lysed with ice-cold RIPA buffer (50 mM Tris-Cl, pH 8.0, 150 mM NaCl, 1% Nonidet P-40, 0.1% sodium dodecyl sulfate, 0.5% sodium deoxycholate, protease inhibitors, and phosphatase inhibitors). The samples were separated by 10% sodium dodecyl sulfate-polyacrylamide gel electrophoresis (PAGE) and transferred to a PVDF membrane (Bio-Rad, Hercules, CA). Membranes were blocked with 5% non-fat milk and then incubated with anti-HSD17B4 (1:250, HPA021302; Atlas Antibodies, Stockholm, Sweden), anti-PMP70 (1:500, SAB4200181; Sigma-Aldrich, St. Louis, MO), anti-ß-actin (1:2000, sc-47778; Santa Cruz Biotechnology, Dallas, TX), and anti-α tubulin (1:25000, 11224-1-AP; Proteintech, Rosemont,

Figure 1 Identification of mutations in HSD17B4, encoding DBP, in families with SCAR

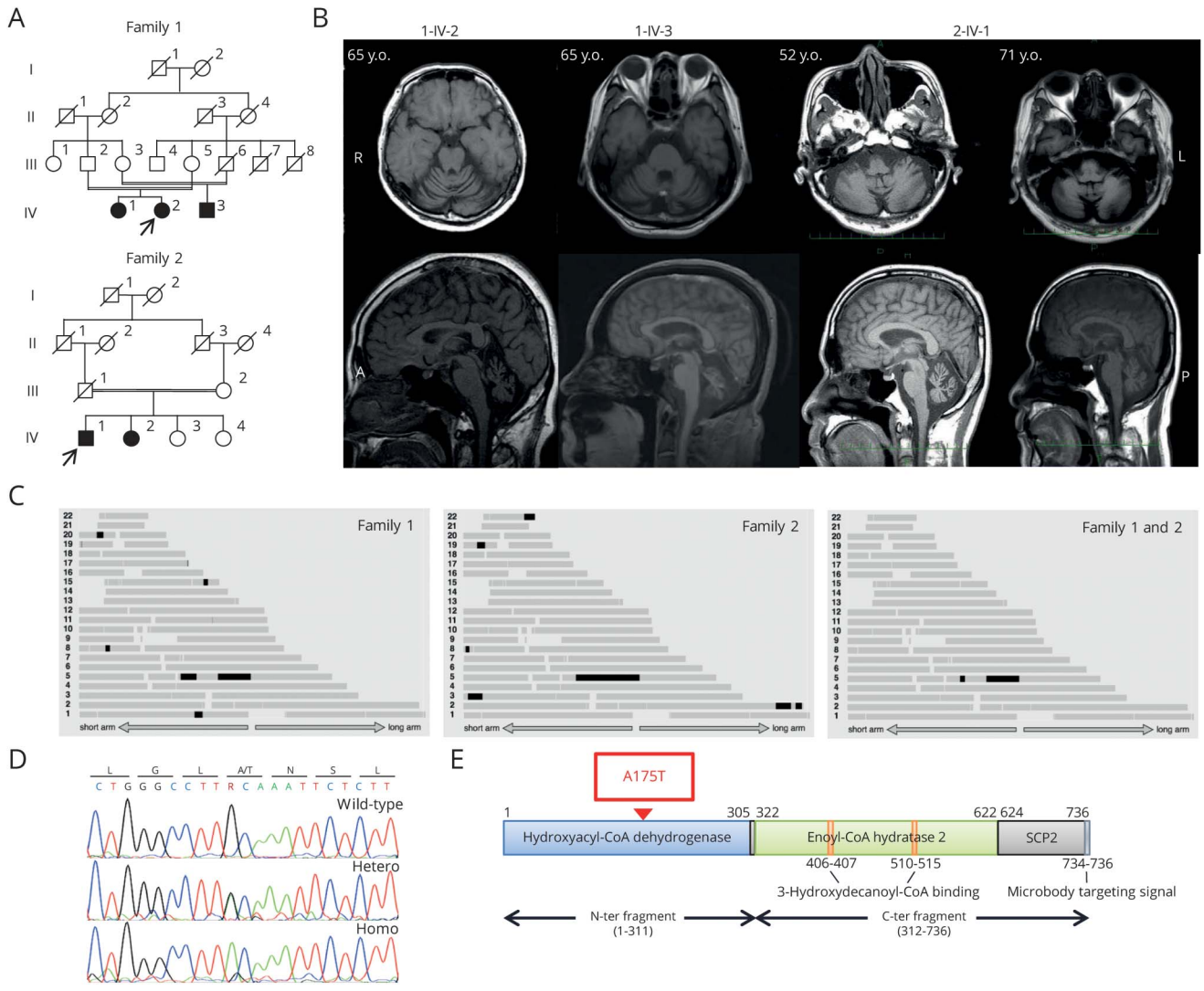

(A) Pedigrees in families 1 and 2, both of which had consanguineous marriages. Affected individuals are indicated by filled circles or squares. (B) Brain MRI of 3 patients (1-IV-2 at age 65 years, 1-IV-3 at age 65 years, and 2-IV-1 at ages 52 and 71 years): upper, T1-weighted axial images; lower, T1-weighted sagittal images. Cerebellar atrophy was observed. (C) Homozygosity fingerprinting of 4 individuals (family 1, 1-IV-2 and 1-IV-3; family 2, 2-IV-1 and 2-IV-2). Black bars indicate IBD. Relatively long segments of IBD were found in chromosome 5. (D) Sanger sequencing of mutations in HSD17B4 of a patient (2-IV-2); her unaffected sister was used as a control (2-IV-3). The mutation segregated with the phenotype in the family members. (E) Domain architecture of DBP with the mutation. DBP = D-bifunctional protein; IBD = identity by descent; SCAR = spinocerebellar ataxia, autosomal recessive.

IL) primary antibodies. The immunoreactive bands were detected with LAS-4000 (GE Healthcare, Chicago, IL). The quantitative densitometric analyses were performed with Image Quant LAS 4000 software (GE Health care). Blue native PAGE (BN-PAGE) analysis was performed using the NativePAGE Novex Bis-Tris Gel System (Life Technologies, Carlsbad, CA). We used the NativePAGE 4–16% Bis-Tris Protein Gel (Life Technologies). Fibroblasts were lysed with ice-cold lysis buffer (50 mM bis-tris [HCl], pH 7.2, 50 mM NaCl, 10% glycerol, 0.001% Ponceau S, 1% digitonin, protease inhibitors, and phosphatase inhibitors).

Quantitative reverse transcription PCR

Total RNA was extracted from fibroblasts using the RNeasy Mini Kit (Qiagen, Hilden, Germany). Complementary DNA was generated using oligo-d(T) primers and the ReverTra-Plus kit (Toyobo, Osaka, Japan). Quantitative real-time expression analysis was performed using THUNDERBIRD SYBR qPCR Mix (Toyobo) on the StepOnePlus Real-Time PCR system (Thermo Fisher Scientific). We used the standard curve quantification method with *GAPDH* as the reference gene. Primers are as follows: GAPDH-Fw, GAAGGTGAAGGTCGGAGTCAACG; GAPDH-Rv, GAAGATGGTGATGGGATTTCC; HSD17B4-Fw, AGTTGCTTTTGATAGGTGCAG; and HSD17B4-Rv, AAAGCTCATTCCACATAGGTTTG.

Immunocytochemistry and confocal microscopy

Fibroblasts were fixed with 4% paraformaldehyde and stained with anti-HSD17B4 (1:50, HPA021302; Atlas Antibodies) and

Table 1 Clinical and pathophysiologic features of DBP deficiencies grouped by age at onset

	Infant onset	Juvenile onset	Adult onset
Onset	**<2 y**	**2–20 y**	**>20 y**
Clinical feature			
Cortical malformations	++	+	–
Hepatomegaly	+	–	–
Infertility	NA	++	+
Seizure	+	–	–
Intellectual disability	++	+	–
Late language acquisition	++	++	–
Visual loss	+	+	–
Nystagmus	NA	++	++
Saccadic eye movement	NA	++	++
Hearing loss	++	++	++
Dysarthria	NA	++	++
Dysphagia	NA	–	+
Pyramidal sign	NA	+	–
Spasticity	–	+	–
Cerebral hypotonia	++	–	–
Cerebellar hypotonia	–	–	+
Truncal ataxia	NA	++	++
Limb ataxia	NA	++	++
Tremor	–	+	++
Peripheral neuropathy	++	++	++
Impaired vibratory sense	NA	+	++
Progression	Rapid	Slow	Slow
MRI			
White matter lesion	++	+	–
Cerebellar atrophy	++	++	++
Laboratory data			
VLCFA in blood	↑	→	→
DBP enzymatic activity	↓↓	↓	NA
mRNA expression of DBP	↓↓	↓	→
Protein expression of DBP	↓↓↓	↓↓	↓

Abbreviations: – = absent; + = present in some cases; ++ = present in most cases; DBP = D-bifunctional protein; mRNA = messenger RNA; NA = not assessed; VLCFA = very-long-chain fatty acid.

anti-PMP70 (1:250, SAB4200181; Sigma-Aldrich) antibodies. Anti-rabbit IgG Alexa Fluor 594 and anti-mouse IgG Alexa Fluor 488 (1:500; Thermo Fisher Scientific) were used as secondary antibodies. Immunostained cells were examined using a confocal microscope (LSM800; Carl Zeiss, Jena, Germany). Intensities were analyzed using ImageJ.

In silico modeling

Three-dimensional experimental structures were retrieved from the Protein Data Bank (PDB) and analyzed with PyMOL.

Collection of clinical data and pathogenicity scoring

Previously reported mutations and clinical data were collected from the literature[4–11,18–24] and ClinVar. Mutations were used if they were reported with sufficient clinical detail. Selected mutations were divided into 3 groups based on age at onset (table 1): infant onset, under 2 years; juvenile onset, from 2 to 19 years; and adult onset, over 20 years. The pathogenicity of the mutations was assessed with CADD.

Statistics

Numerical data are indicated as the mean ± standard error of mean or as the mean ± SD. The Student *t* test was used for statistical analysis in immunocytochemical experiments. The Tukey HSD test was used in Western blotting and quantitative reverse transcription PCR (RT-qPCR) experiments. Differences in CADD scores among the 3 groups were assessed with the Kruskal-Wallis test. The level of significance was set at $p < 0.05$.

Data availability

The protocol and the statistical analysis plan are available on request.

Results

Clinical description

The 2 affected individuals of family 1 (1-IV-1 and 1-IV-2) were born from consanguineous parents. Neither had motor function abnormalities during their childhood. The older sister (1-IV-1) developed gait disturbance at age 33 years and the younger sister (1-IV-2) at age 35 years, whereas previously reported patients with adult-onset DBP deficiency developed ataxia by age 30 years. The younger woman had 2 miscarriages and secondary amenorrhea at age 35 years, and neither patient had any children. She developed hearing loss in her 30s and dysarthria at age 38 years and experienced difficulty writing at age 39 years. Her cognitive function was normal. She exhibited horizontal nystagmus and saccadic eye movement without limitations. Although dysarthria was observed, there was no obvious dysphagia. Other neurologic symptoms included severe bilateral sensorineural hearing loss, ataxia of the upper and lower limbs, and difficulty transferring from sit to stand and walking. Observed reflexes were normal, and no abnormalities

of the sensory system or autonomic nervous system were observed. Progression of the cerebellar ataxia was very slow. She was able to walk without assistance until age 66 years when she began using a wheelchair. This is much later than other patients with adult-onset DBP deficiency who require wheelchairs by their 30s. MRI of the brain indicated mild cerebellar atrophy without midbrain and pons atrophy (figure 1B). The symptoms of the older sister were similar to those of the younger one. A cousin of the affected sisters was a male offspring of family 1 (1-IV-3). He was also born from consanguineous parents. No abnormalities in motor function were observed in his childhood. He developed gait disturbance at age 39 years. He has one healthy son. His symptoms progressed slowly, and he began using a wheelchair in his 60s. His neurologic findings showed horizontal nystagmus and saccadic eye movement without limitations. He exhibited ataxia in the upper and lower limbs, action tremor, and terminal tremor, but no muscle weakness or sensory disturbances. His clinical diagnosis is slowly progressive spinocerebellar degeneration. MRI of the brain showed cerebellar atrophy (figure 1B).

The male patient of family 2 (2-IV-1) was a son of neurologically healthy, consanguineous parents. He was aware of mild deafness at age 40 years. His age at onset of ataxia was 49 years. His initial symptoms were gait disturbance and dysarthria. He exhibited neuronal hearing loss in both ears, mild dysarthria, upper and lower limb and trunk ataxia, terminal tremor, and decreased sensation of vibration in the lower limbs. MRI of the brain indicated mild progressive cerebellar atrophy without pons atrophy (figure 1B). Biochemical examinations were performed: plasma levels of VLCFAs were normal; the C24:0/C22:0 ratio was 0.687 (mean = 1.05, SD =

Figure 2 Expression of HSD17B4 transcripts and proteins

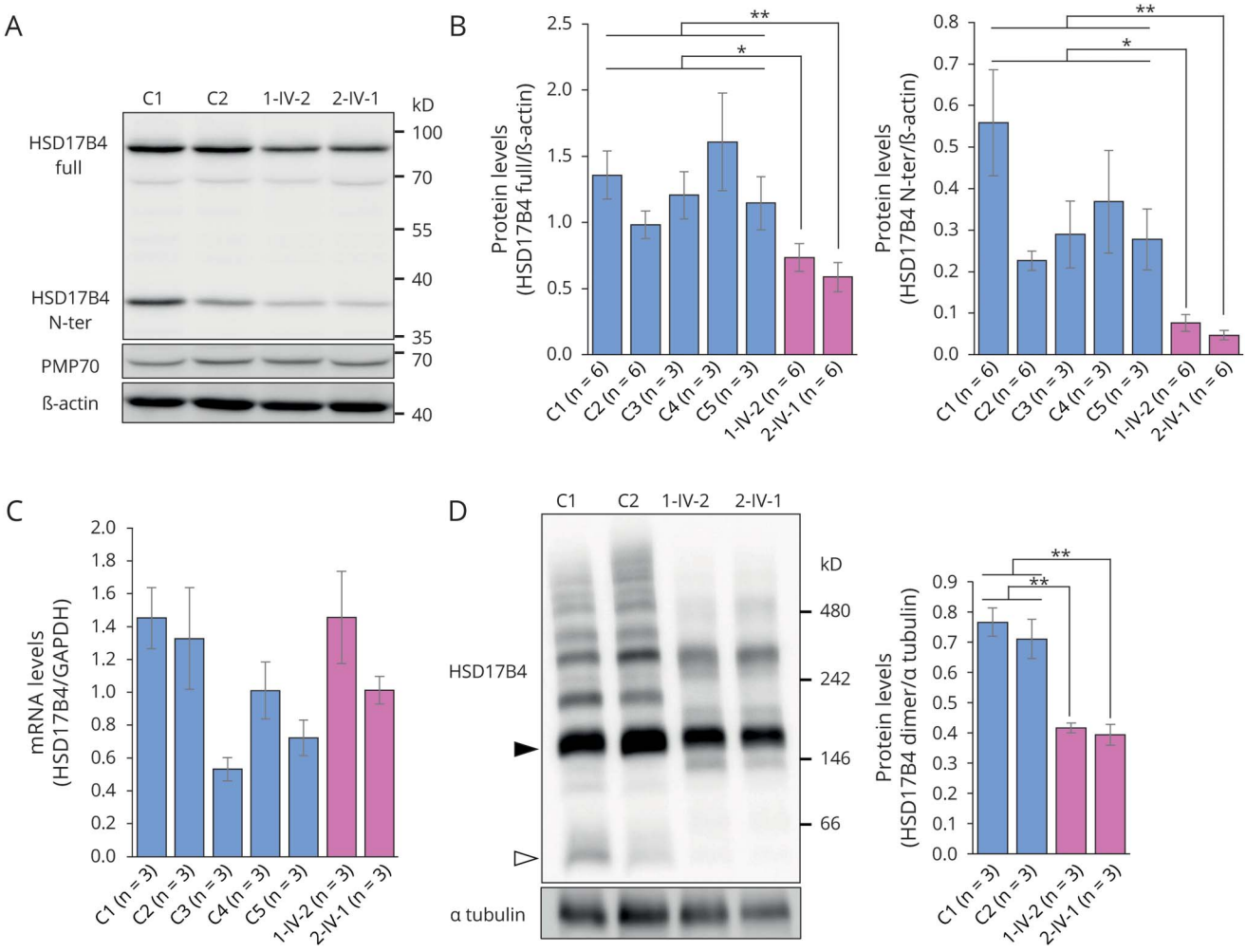

(A and B) Western blotting of lysates from the patients' fibroblasts (1-IV-2 and 2-IV-1) and the healthy controls. (C) Quantitative reverse transcription PCR. The expression level of the mRNA in the patients (1-IV-2 and 2-IV-1) was not different from that of the healthy controls. (D) Dimerized DBP of the patients' fibroblasts (1-IV-2 and 2-IV-1) was reduced in comparison with that of the healthy controls. Fibroblasts were solubilized with 1% digitonin and then analyzed by blue native-polyacrylamide gel electrophoresis followed by immunoblotting using anti-HSD17B4 and anti-α tubulin antibodies. Twenty-five micrograms per lane samples were loaded. The solid arrow indicates the dimerized DBP, and the open arrow shows the processed N-term fragment monomer. Molecular weight markers are shown on the right. Bar graph showed quantification of the level of HSD17B4 protein dimer using that of α tubulin as a loading control. Mean ± SEM. All experiments were repeated 3 or more times. *$p < 0.05$, **$p < 0.01$ DBP = D-bifunctional protein; mRNA = messenger RNA.

Figure 3 Confocal images of fibroblasts

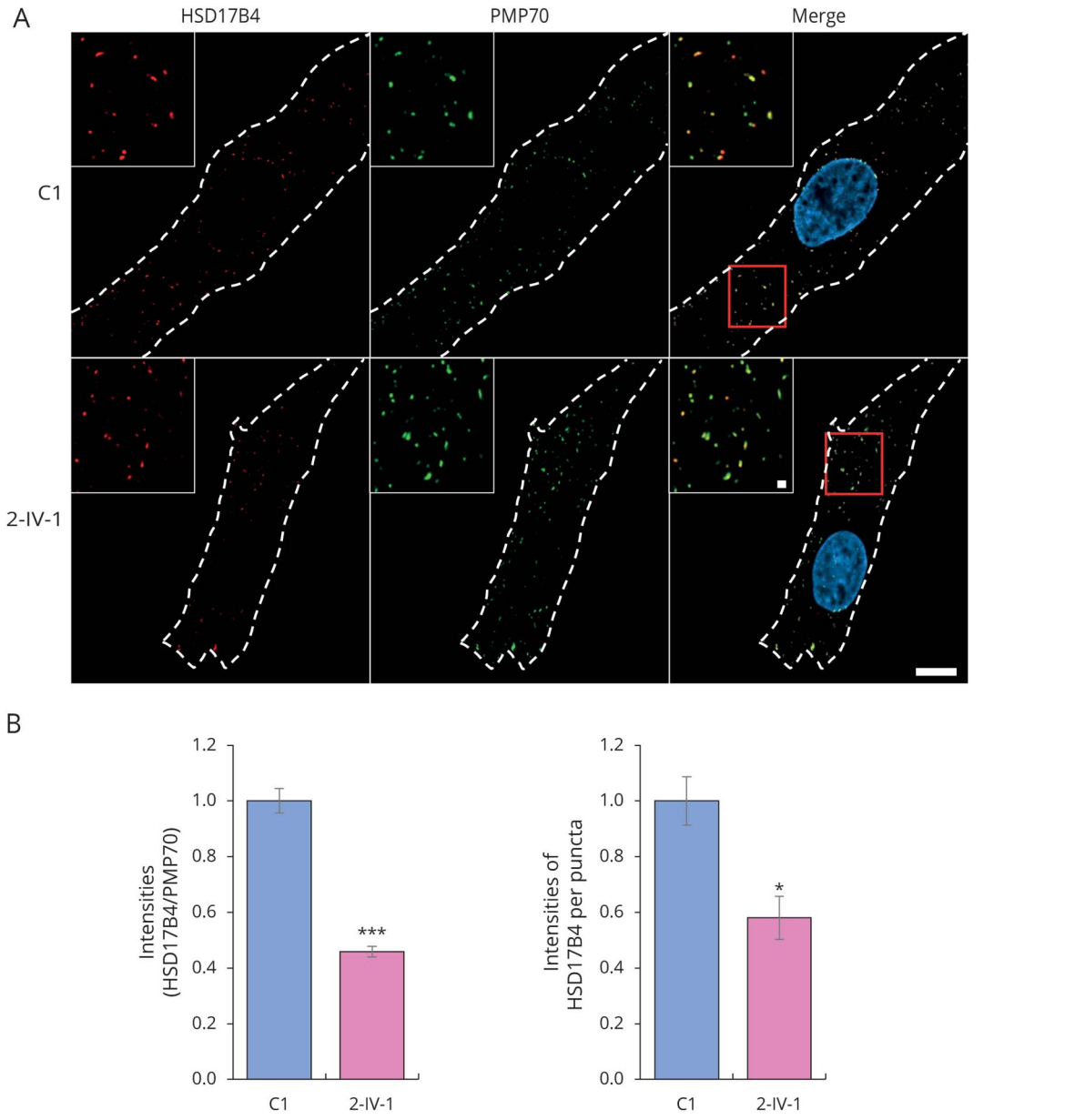

(A) Fibroblasts from a patient (1-IV-2) and a healthy control were immunostained with anti-HSD17B4 antibodies (red), anti-PMP70 (green) as a peroxisome marker, and DAPI (blue). The white dotted lines show the morphology of the fibroblasts. Scale bar is 20 μm. Enlarged images of the red boxed region are also shown in the upper left (scale bar is 1 μm). (B) Quantification of the intensities of HSD17B4 staining compared with PMP70 and of the intensities of HSD17B4 protein per puncta (n = 5 cells each). *$p < 0.05$, ***$p < 0.0001$. DAPI = 4′,6-diamidino-2-phenylindole

0.16); and the C26:0/C22:0 ratio was 0.028 (mean = 0.012, SD = 0.005). His sister (2-IV-2) was also affected and showed similar symptoms. Her age at onset of ataxia was 40 years, and she presented with the initial symptom of intention tremor. The patient developed hearing loss at age 46 years. She also exhibited slurred speech, neck tremor, titubation, and decreased sensation of vibration in the lower limbs. She had no nystagmus apart from saccadic eye movement. Although she had 2 sons, her age at menopause was 33 years. She was able to walk without assistance until she was age 60 years.

Homozygous mutation identification

From the result of homozygosity fingerprinting, a relatively long IBD segment existed in chromosome 5 in both families (figure 1C). Furthermore, as the haplotypes of both families were shared, they may have been derived from the same ancestor. Exome sequencing identified 15 and 5 variants in each family, which were estimated to be pathogenic by at least one of the 3 prediction algorithms. Only one mutation was a common variant in both families: Chr5:118814617G>A corresponding to *HSD17B4* (NM 000414):c.523G>A, p.Ala175Thr (figure 1, D and E). The mutation was located in

the dehydrogenase domain of DBP (figure 1E). Other mutations reported as causative genes of SCAR were not detected. Therefore, we concluded that *HSD17B4* was the most likely candidate. The CADD score of p.Ala175Thr was 11.6. Although p.Ala175Thr was previously reported as one of the compound heterozygous mutations (p.Arg132Trp/p.Ala175Thr),[7] our case with a homozygous p.Ala175Thr mutation is very rare.

Reduction of the level of HSD17B4 proteins despite normal messenger RNA expression

We used an immunoblot assay to examine the expression of the HSD17B4 protein in our patients. Because the epitope of the anti-HSD17B4 antibody is at the N-terminal region of the protein (5–91aa), the antibody recognizes the full-length and the N-terminal 35 kD fragment of the protein. The full-length protein was significantly diminished relative to that of controls (~40%) (figure 2, A and B). The processed 35 kD dehydrogenase domain was also decreased (~70%) (figure 2, A and B). RT-qPCR indicated no reduction in the levels of the transcripts (figure 2C). These results indicate that the steady-state level of the protein was reduced. Moreover, the ratios of HSD17B4 protein expression to PMP70, a peroxisome membrane protein, were decreased (figure e-1, links.lww.com/NXG/A216).

Distribution and quantification of HSD17B4 proteins in the patients' fibroblasts

We stained fibroblasts using anti-HSD17B4 and anti-PMP70 antibodies (figure 3A). HSD17B4 proteins were localized to the peroxisomes in both controls and patients. HSD17B4 was significantly decreased in the patients (figure 3B).

Reduction in the dimerized HSD17B4

Dimerization of HSD17B4 proteins is required for its enzymatic activity.[25] We analyzed the levels of dimerized HSD17B4 proteins in fibroblasts by using BN-PAGE (figure 2D). Dimerized proteins in the patients were significantly reduced relative to those in the healthy controls (~40%). The pattern of oligomers differed between patients and controls.

Structure modeling by A175T mutation

p.Ala175 is conserved only among humans, gorillas, lizards, medakas, and zebrafish. The alanine residue found in these species is replaced with a cysteine or serine in other species (figure 4A). The crystal structure of the dehydrogenase domain of human HSD17B4 (PDB: 1ZBQ) was used to assess the potential effects of the mutations (figure 4B). The side chain of Ala175 is situated on the outer surface of the dimerized α helix.[26] Unlike variants of cysteine or serine residues, mutation of a threonine residue results in an increased side chain volume and consequently altered packing that might affect the homodimer interaction (figure 4C). Although the mutations do not directly affect residues in the active site, they potentially alter the stability of the dimer.

Comparison between mild A175T-induced symptoms and reports of severe mutations

We calculated the CADD scores of the *HSD17B4* mutations previously reported and compared the scores of the 3 groups based on age at onset (figure 5 and table e-1, links.lww.com/NXG/A217). The CADD scores of the severe phenotypes

Figure 4 Three-dimensional structure of the dehydrogenase domain

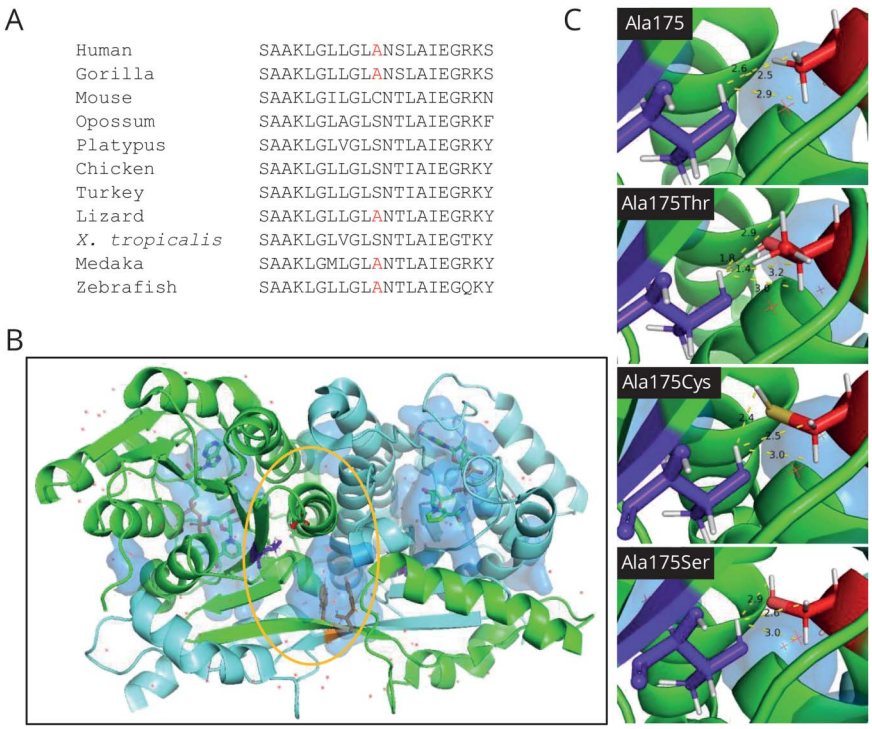

(A) Conservation of the protein sequence at the mutation. Mutated residue is in red. (B) Crystal structure of the homodimeric dehydrogenase domain complex of DBP, taken from the Protein Database (id, 1ZBQ). Circle: dimerized region. (C) Magnification around Ala175 residue. The side chains of the Ala175 residue (red) and Thr191 residue are shown (purple). The side chain of Ala175Thr is closest to that of Thr191. The calculated black value (Å) indicates the distance between side chains having hydroxyl groups. This model shows the most frequent structure. DBP = D-bifunctional protein.

tended to be higher than the milder ones. A mutation of p.Ala175Thr featured the lowest CADD score. The onset age of our patients was from 33 to 49 years, which encompasses older ages than those considered by previous reports. There was a tendency to be associated between CADD score and age at onset ($p = 0.01$).

Discussion

Our study is the report on middle age–onset DBP deficiency and revealed that *HSD17B4*, a causative gene of DBP deficiency, induced a middle age–onset slowly progressive SCAR. We also obtained biochemical, immunocytochemical, and structural modeling data to confirm the pathophysiology. Moreover, by comparing with previous data, we indicated that CADD scores may be used to estimate the severity of a DBP deficiency.

Two families were independently screened for a genetic mutation associated with SCAR. *HSD17B4* was the only common candidate for both families and was located in the IBD segment with the shared haplotype. The CADD score of the p.Ala175Thr mutation was low. However, the p.Ala175Thr mutation was previously reported as a compound heterozygous mutation.[7] We conducted the following analysis to investigate the pathogenicity of p.Ala175Thr homozygous mutation of *HSD17B4*.

First, we performed an in vitro assay with fibroblasts. Although the abundance of the DBP protein was reduced, the expression of the messenger RNA (mRNA) was normal. In addition, although DBP protein localization in peroxisomes was normal, the amount of DBP in the peroxisomes decreased. Moreover, the BN-PAGE analysis revealed that levels of dimerized DBP, the protein's functional form, were diminished in the patients. These data indicate that the steady-state level of DBP protein was impaired. Next, structural modeling assessment also suggests that p.Ala175Thr potentially affects the dimerization of DBP. Thus, the quantitative reduction in functional DBP in the patients could explain the pathogenicity of the homozygous *HSD17B4* mutation.

The main clinical features of our patients were cerebellar ataxia, sensorineural hearing loss, and mild peripheral neuropathy. In these patients, disease onset occurred in middle age, which was an older onset age than that described in previous reports. We compared the symptoms exhibited by our patients with those of previously reported patients and classified the cases into 3 groups according to the age of DBP deficiency onset (table 1). Our cases were included in the adult-onset group. The infant-onset group shows the most severe clinical features and death before age 2 years and is characterized by cortical malformation, seizure, hepatomegaly, and hypotonia. Some patients with infant-onset DBP deficiency exhibit milder features, primarily linked to leukodystrophies, which permit survival into childhood. In contrast, juvenile- and adult-onset groups are much milder than infant onset. Unlike infant onset, juvenile and adult onset have cerebellar ataxia as the main symptom. Although there are some similarities between both juvenile- and adult-onset groups, notable differences exist. Intellectual disability, retinopathy, and pyramidal signs are seen in many cases of juvenile onset, whereas pure cerebellar ataxia, in addition to deafness, tends to be observed in most cases of adult onset. Infertility in the adult-onset group is milder and less frequent than in the juvenile-onset group. A few cases of adult onset present intellectual disability, but these symptom seems to be caused by hearing loss.

As mentioned above, we performed biochemical analyses and compared the results with previous reported data. The infant-

Figure 5 Relationship between predicted pathogenicity of mutations and age at onset

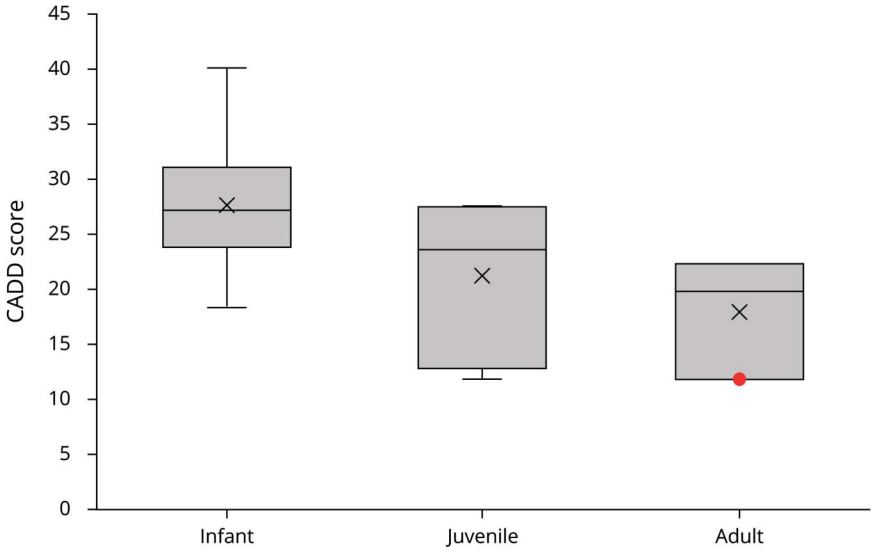

Graph showing the distribution of the age at onset of the DBP deficiency (infant [n = 36], juvenile [n = 6], and adult [n = 3]) from this study and previous literature. The score of p.Ala175Thr is indicated as a red dot. CADD = Combined Annotation-Dependent Depletion; DBP = D-bifunctional protein.

onset group features depletion of both the HSD17B4 protein and mRNA expression.[18,27] In relatively mild cases of infant-onset, RNA expression was significantly lower than that in controls; patients with severe disease exhibited even lower levels of RNA expression.[27] In both severe and mild cases of infant onset, the proteins were not detected. Even among cases of infant onset, a slight residual DBP could account for the survival of the patients.[18] In vivo experiments provide additional supporting evidence that knock-out mice show severe growth retardation during the first weeks of life, resulting in the premature death of one-third of the affected mice.[28] In juvenile-onset DBP deficiency, a remarkable reduction in HSD17B4 mRNA and protein has been observed in patients' fibroblasts and lymphoblasts and overexpressed HEK293T cells with a mutant *HSD17B4*.[4,8,9,11] In adult-onset cases, the levels of mRNA expression were normal, and the expression levels of DBP remained moderate. The impaired enzyme activities result from dysfunction or reduction of the protein, but our data suggest that the delayed onset of disease may be attributed to the remaining DBP protein function. These pathophysiologic features could represent differences in the 3 groups based on age at onset.

The pathogenicity of the identified mutation was evaluated in each age-onset group with CADD, and the scores of each of the 3 groups were compared (figure 5). We analyzed the correlation with the age at onset using the average CADD score of both alleles and the lower CADD score. The lower CADD scores were more associated with disease severity. The CADD score of the identified mutation, Ala175Thr, was low, which is consistent with the milder symptom severity presented in the older-onset group. Therefore, CADD scores could estimate the severity of the DBP deficiency with a certain degree of accuracy.

Our results indicate that a homozygous mutation of *HSD17B4* was responsible for slowly progressive SCAR. The data on the oldest cases of DBP deficiency hitherto reported broaden the scope of DBP deficiency phenotypes.

Acknowledgment

The authors thank the families involved in this research and Dr. Akiko Ohtake and Ms. Eiko Nakajima for the technical assistance.

Study funding

This work was supported by Grants-in-Aid for JSPS Research Fellow 16J40095 (Y. Matsuda), JSPS KAKENHI Grant 26893162 (Y. Matsuda), 15K15083 (H. Morino), and 26242085 (H. Kawakami), and the Takeda Science Foundation (H. Kawakami).

Disclosure

Disclosures available: Neurology.org/NG.

Publication history

Received by *Neurology: Genetics* May 3, 2019. Accepted in final form November 19, 2019.

Appendix Authors

Name	Location	Role	Contribution
Yukiko Matsuda, PhD	Research Institute for Radiation Biology and Medicine, Hiroshima University, and Japan Society for the Promotion of Science, Tokyo	Author	Study concept and design, data acquisition, analysis, and interpretation, and manuscript preparation and revision
Hiroyuki Morino, MD, PhD	Research Institute for Radiation Biology and Medicine, Hiroshima University	Author	Study concept and design, data acquisition, analysis, and interpretation, and manuscript revision
Ryosuke Miyamoto, MD	Institute of Biomedical Sciences, Tokushima University Graduate School	Author	Data acquisition and patient evaluation
Takashi Kurashige, MD, PhD	National Hospital Organization Kure Medical Center	Author	Sample collection and manuscript revision
Kodai Kume, MD, PhD	Research Institute for Radiation Biology and Medicine, Hiroshima University	Author	Interpretation and manuscript revision
Noriyoshi Mizuno, DDS, PhD	Graduate School of Biomedical & Sciences, Hiroshima University	Author	Interpretation and manuscript revision
Yuhei Kanaya, MD	Research Institute for Radiation Biology and Medicine, Hiroshima University	Author	Interpretation and manuscript revision
Yui Tada, MS	Research Institute for Radiation Biology and Medicine, Hiroshima University	Author	Interpretation and manuscript revision
Ryosuke Ohsawa, PhD	Research Institute for Radiation Biology and Medicine, Hiroshima University	Author	Interpretation and manuscript revision
Kazunori Yokota, MD, PhD	Hiroshima University Hospital	Author	Sample collection
Nobuyuki Shimozawa, MD, PhD	Life Science Research Center, Gifu University	Author	Data analysis
Hirofumi Maruyama, MD, PhD	Hiroshima University	Author	Interpretation and manuscript revision
Hideshi Kawakami, MD, PhD	Research Institute for Radiation Biology and Medicine, Hiroshima University	Author	Study concept, design, and manuscript revision

References

1. Ferdinandusse S, Denis S, Mooyer PA, et al. Clinical and biochemical spectrum of D-bifunctional protein deficiency. Ann Neurol 2006;59:92–104.
2. Gloerich J, Denis S, Van Grunsven EG, et al. A novel HPLC-based method to diagnose peroxisomal D-bifunctional protein enoyl-CoA hydratase deficiency. J Lipid Res 2003;443:640–644.
3. Wanders RJA, Barth PG, Heymans HAS. Single peroxisomal enzyme deficiencies. In: Scriver CR, Beaudet AL, Sly WS, Valle D, editors. The Molecular and Metabolic Bases of Inherited Disease. New York: Mc-Graw-Hill,; 2001:3219–3256.

4. Amor DJ, Marsh AP, Storney E, et al. Heterozygous mutations in *HSD17B4* cause juvenile peroxisomal D-bifunctional protein deficiency. Neurol Genet 2016;2: e114.
5. Lieber DS, Hershman SG, Slate NG, et al. Next generation sequencing with copy number variant detection expands the phenotypic spectrum of HSD17B4-deficiency. BMC Med Genet 2014;15:30.
6. Lines MA, Jobling R, Brady L, et al. Peroxisomal D-bifunctional protein deficiency: three adults diagnosed by whole-exome sequencing. Neurology 2014;82:963–968.
7. Matsukawa T, Koshi KM, Mitsui J, et al. Slowly progressive D-bifunctional protein deficiency with survival to adulthood diagnosed by whole-exome sequencing. J Neurol Sci 2017;372:6–10.
8. McMillan HJ, Worthylake T, Schwartzentruber J, et al. Specific combination of compound heterozygous mutations in 17ß-hydroxysteroid dehydrogenase type 4 (*HSD17B4*) defines a new subtype of D-bifunctional protein deficiency. Orphanet J Rare Dis 2012;7:90.
9. Chen K, Yang K, Luo SS, et al. A homozygous missense variant in HSD17B4 identified in a consanguineous Chinese Han family with type II Perrault syndrome. BMC Med Genet 2017;18:91.
10. Demain LA, Urquhart JE, O'Sullivan J, et al. Expanding the genotypic spectrum of Perrault syndrome. Clin Genet 2017;91:302–312.
11. Pierce SB, Walsh T, Chisholm KM, et al. Mutations in the DBP-deficiency protein HSD17B4 cause ovarian dysgenesis, hearing loss, and ataxia of Perrault syndrome. Am J Hum Genet 2010;87:282–288.
12. Hagiwara K, Morino H, Shiihara J, et al. Homozygosity mapping on homozygosity haplotype analysis to detect recessive disease-causing genes from a small number of unrelated, outbred patients. PLoS One 2011;6:e25059.
13. Morino H, Miyamoto R, Ohnishi S, et al. Exome sequencing reveals a novel TTC19 mutation in an autosomal recessive spinocerebellar ataxia patient. BMC Neurol 2014; 14:5.
14. Ramensky V, Bork P, Sunyaev S. Human non-synonymous SNPs: server and survey. Nucleic Acids Res 2002;30:3894–3900.
15. Ng PC, Henikoff S. Predicting deleterious amino acid substitutions. Genome Res 2001;11:863–874.
16. Schwarz JM, Rödelsperger C, Schuelke M, Seelow D. MutationTaster evaluates disease-causing potential of sequence alterations. Nat Methods 2010;7:575–576.
17. Rentzsch P, Witten D, Cooper GM, et al. CADD: predicting the deleteriousness of variants throughout the human genome. Nucleic Acids Res 2019;47:D886–D894.
18. Ferdinandusse S, Ylianttila MS, Gloerich J, et al. Mutational spectrum of D-bifunctional protein deficiency and structure-based genotype-phenotype analysis. Am J Hum Genet 2006;78:112–124.
19. Konkol'ová J, Petrovič R, Chandoga J, et al. Peroxisomal D-bifunctional protein deficiency: first case reports from Slovakia. Gene 2015;568:61–68.
20. Nakano K, Zhang Z, Shimozawa N, et al. D-bifunctional protein deficiency with fetal ascites, polyhydramnios, and contractures of hands and toes. J Pediatr 2001;139: 865–867.
21. Nascimento J, Mota C, Lacerda L, et al. D-bifunctional protein deficiency: a cause of neonatal onset seizures and hypotonia. Pediatr Neurol 2015;52:539–543.
22. Tsuchida S, Osaka A, Abe Y, et al. Effects of naturally occurring missense mutations and G525V in the hydratase domain of human d-bifunctional protein on hydratase activity. Mol Genet Metab Rep 2014;2:41–45.
23. van Grunsven EG, van Berkel E, Ijlst L, et al. Peroxisomal D-hydroxyacyl-CoA dehydrogenase deficiency: resolution of the enzyme defect and its molecular basis in bifunctional protein deficiency. Proc Natl Acad Sci USA 1998;95:2128–2133.
24. Yubero D, Brandi N, Ormazabal A, et al. Targeted next generation sequencing in patients with inborn errors of metabolism. PLoS One 2016;11:e0156359.
25. Haataja TJ, Koski MK, Hiltunen JK, Glumoff T. Peroxisomal multifunctional enzyme type 2 from the fruitfly: dehydrogenase and hydratase act as separate entities, as revealed by structure and kinetics. Biochem J 2011;435:771–781.
26. Mehtälä ML, Lensink MF, Pietikuäinen LP, et al. On the molecular basis of D-bifunctional protein deficiency type III. PLoS One 2013;8:e53688.
27. Mizumoto H, Akashi R, Hikita N, et al. Mild case of D-bifunctional protein deficiency associated with novel gene mutations. Pediatr Int 2012;54:303–304.
28. Baes M, Huyghe S, Carmeliet P, et al. Inactivation of the peroxisomal multifunctional protein-2 in mice impedes the degradation of not only 2-methyl-branched fatty acids and bile acid intermediates but also of very long chain fatty acids. J Biol Chem 2000; 275:16329–16336.